Bulletin of Environment, Pharmacology and Life Sciences
Bull. Env. Pharmacol. Life Sci., Vol 12 [10] September 2023 : 128-139

Online ISSN 2277-1808
Journal's URL:http://www.bepls.com
CODEN: BEPLAD

ORIGINAL ARTICLE **OPEN ACCESS**

SPIHT Image Compression Algorithm for High-Precision Digital Images

Goh Jee Yuan[1], Afzan Adam[1]*, Mohammad Kamrul Hasan[2¶], AKM Ahasan Habib[2¶], Zaid Abdi Alkareem Alyasseri[3¶], Mohammad Faizal Ahmad Fauzi[4&], Elaine Wan Ling Chan[5&]

[1]Center for Artificial Intelligence Technology, Faculty of Information Science and Technology, 43300, Universiti Kebangsaan Malaysia, Malaysia.

[2]Center for Cyber Security, Faculty of Information Science and Technology, 43300, Universiti Kebangsaan Malaysia, Malaysia

[3]Information Technology Research and Development Center, University of Kufa, Najaf, Iraq.

[4]Faculty of Engineering, Multimedia University, Jalan Multimedia, 63100 Cyberjaya, Selangor, Malaysia

[5]The Institute for Research, Development and Innovation, International Medical University, 57000 Kuala Lumpur, Malaysia

*Corresponding Author: Email: afzan@ukm.edu.my

¶ These authors contributed equally to this work and, & these authors also contributed equally to this work

ABSTRACT

The improvement of digital imaging technologies has contributed to the acquisition of high-resolution medical images and, at the same time, caused exponentially increasing file sizes. Several studies have reported using the Set Partitioning in Hierarchical Trees (SPIHT) algorithm as the state-of-the-art in near-lossless image compression; however, the use of the SPIHT algorithm in the compression of high-resolution whole pathology slide scans (also known as digital slides) remains to be accomplished. Thus, this research aims to investigate the performance of the SPIHT image compression algorithm when applied on digital slides and then to propose an improved near-lossless auto-recursive SPIHT-based image compression algorithm. A total of 50 pathology glass slides of blood smear, prostate, breast, and cervical cancer were collected with assistance from Hospital Canselor Tuanku Muhriz UKM (HCTM) to form the data set used for this research. Preliminary experimentation is carried out by applying image compression on a set of medical images using different algorithms to assess how each algorithm performs against the SPIHT algorithm. Then different wavelets are tested with SPIHT to discover which wavelet used in SPIHT will produce a compressed image with the highest quality. The proposed algorithm is then tested against the original SPIHT algorithm on the dataset, consisting of the digital slides' sub-images. After compression, the proposed algorithm achieved a higher image quality, producing a PSNR of 43.7181 against the original SPIHT algorithm, which only produced a PSNR of 41.1340.
Keyword: PSNR, SPIHT, UKM, Video data.

Received 01 .08.2023 Revised 25.08.2023 Accepted 23 .09.2023

INTRODUCTION

The huge amount of medical information regarding patients that is constantly recorded in hospitals, imaging facilities, and other medical organizations has grown to be a severe problem. Innovative techniques and technologies, including coding methods, are needed in certain applications like medical imaging and real-time transmission to limit the amount of data that needs to be kept or transferred. Without information coding, it is exceedingly difficult and occasionally impossible to create a mechanism to store or transfer big data (huge amounts of complicated, high rates picture, audio, and video data). The unnecessary or redundant details within the original image that the human eye cannot see are removed to obtain the encoding of these data [1-3].

Image compression is a form of data compression applied to digital images to reduce the size of images for storage and transfer. Compression is achieved by using an algorithm on the digital image data that modifies the data to retain a similar visual perception but is reorganized in a more cost-effective storage solution, hence reducing the digital image size [4].

Image compression will be applied to the images by using the SPIHT algorithm, and the resulting images from the compression of the SPIHT algorithm will be compared against the resulting images under other compression algorithms for the same images [5, 6]. The parameters for comparison will include Peak Signal-to-Noise Ratio (PSNR), Structural Similarity Index Measure (SSIM), and also Compression Ratio (CR) [7, 8].

This research aims to apply image compression in the medical field to reduce the size of medical images, which can get very large as the images can have very large dimensions or require very fine attention to small details. This research examines the use of image compression in the field of medicine. It explores how they function to compress whole pathology slide scans and proposes an improved algorithm for the compression of whole pathology slide scans. Although there have been several studies on image compression in medicine, examination of the topic of applying image compression on whole pathology slide scans is still lacking. This research focuses primarily on applying an improved SPIHT-based algorithm by looking into and fine-tuning the algorithm's parameters.

The remainder of this paper is organized as follows: Section 2 presents digital imaging in medicine. Set Partitioning in Hierarchical Trees algorithms discuss in section 3. The SPIHT Algorithm Improvement Results presented in section 4 and section 5 present the conclusion.

Digital Imaging in Medicine

As digital imaging technology improves, many fields enjoy the benefits of the products of technological improvements; one such field would be the field of medicine. Digital imaging methods such as Computed Tomography (CT), Magnetic Resonance Imaging (MRI), and WSI represent digital imaging technology advancements in medicine. These advancements have improved how medical services are prepared and delivered, making them much faster and more efficient. A few examples of digital medical images are shown in Figure 1.

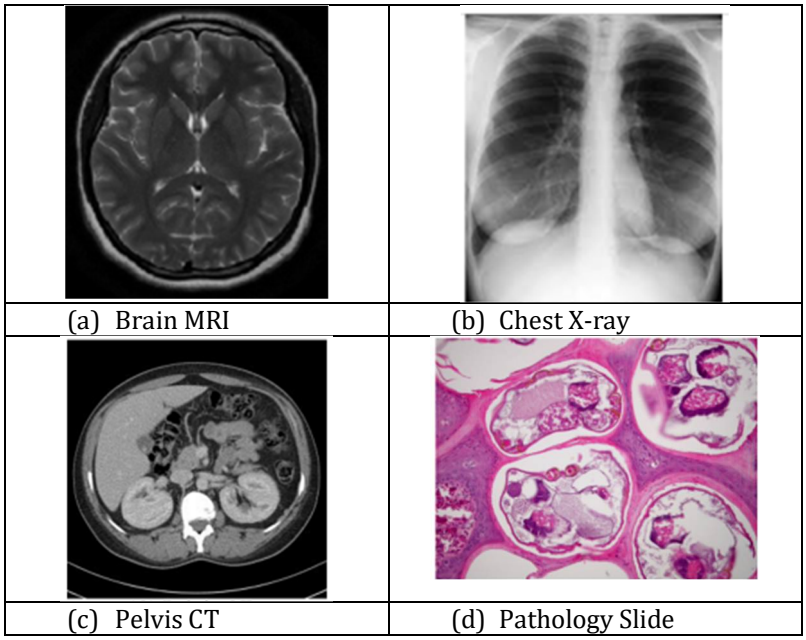

Figure 1. Examples of digital imaging in medicine

Compared to physical images, digital images have the benefit of durability, flexibility, and portability [9]. Digital images are highly durable and much less fragile when compared to physical images, as a digital image can be repeatedly accessed and viewed over a long period on a digital device without any damage to its structural integrity, while a physical image is much more fragile and must be handled with much care to prevent any scratches or tears that might damage the image. Digital images are also highly flexible as copies can be easily made and displayed on drawing tablets, allowing medicinal practitioners to make cites and comments without worrying about damaging the source image.

Digital images are also much more portable and easily transferable to any destination with fast speeds and ease. But as the number of images and data in each image increases exponentially as we enter the digital era, new problems, such as insufficient storage space and slow transfer speeds due to large file sizes, occur. As such, a method to ease the problem is proposed as digital image compression to reduce the storage space and bandwidth needed to store and transfer these digital images.

Whole Slide Imaging: Pathology slide scans refer to scanning a whole glass slide with specialized hardware's assistance to produce a digital copy of the whole slide. These digital copies can then be studied, analyzed, and shared among pathologists, medical, and educational institutes for diagnostic, educational, and research purposes [10]. What sets pathology slide scans apart from CT, X-Ray, and MRI images is the resolution of these images. Pathology slide scans are enormously large in resolution, so large that most common image-viewing software cannot view the entire image. For comparison, CT images have a common resolution of 512*512, 512 pixels in width, and 512 pixels in length. While X-Ray and MRI image resolutions vary from 256*256 to 320*320 pixels. But pathology slide scans can vary from approximately 100,000-110,000 pixels in width and 80,000-90,000 pixels in height. A comparison between the scale of a CT image against a pathology slide scan is illustrated in Figure 2.

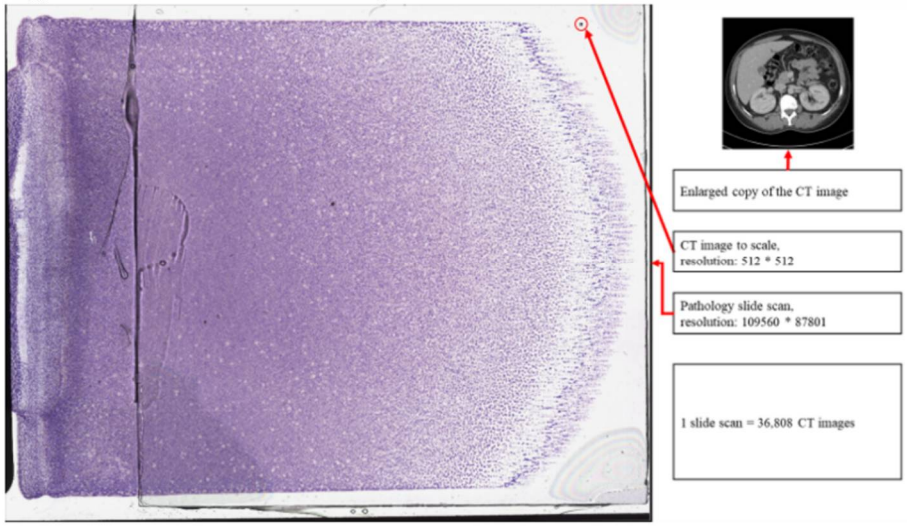

Figure 2. Scaled size comparison of CT image to pathology slide scan

A pathologist looks through the whole slide across different zoom levels to analyze and process the data in each slide. Common levels of magnification that are significant for pathologists when analyzing a slide scan are 4X, 10X, and 40X [10]. The difference in details across multiple zoom levels of the same digital pathology slide are discussed below. In Figure 3a, at 4X magnification or the scanning objective, the pathologist scans through the whole slide while identifying tissues and organs. At this zoom level, we can see the general arrangement pattern of the cells or cell types based on the colors of the cells. An area or areas of study are then determined and selected by the pathologist for further analysis under higher magnification.

Figure 3b, at 10X magnification or the low-power objective, the pathologist focuses on the selected general area of interest for study. At this magnification level, the pathologist can generally analyze the status of the cells in the sample at a good magnification while maintaining a high degree of movement flexibility to move about the region of interest. Once a certain zone or group of cells requires close observation, whether due to the need for closer inspection to obtain finer details or suspicion of abnormal cells, the pathologist will move on to an even higher magnification for further analysis. In Figure 3c, at 40X magnification or the high-power objective, the pathologist focuses on a specific small region or group of cells or a certain individual abnormal cell. At 40X magnification, it is ideal for observing fine details of individual cells, giving the pathologist a detailed image of the specimen in the digital slide.

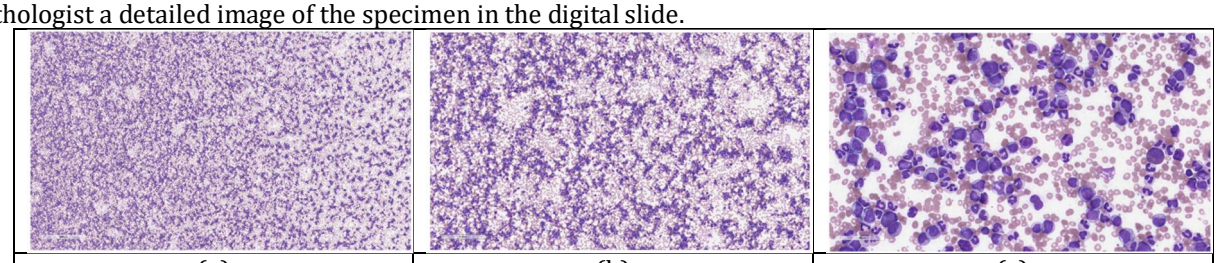

(a) (b) (c)

Figure 3. Digital slide; (a) 4X magnification, with dimensions of 16901*9689 with 500um; (b) 10X magnification, with dimensions of 6761*3876 with 200um ;(c) 40X magnification, with dimensions of 1691*969 with 50um.

Image Compression Techniques: Image compression is done by an encoder, which encodes all the data in an image based on the compression algorithm inputted in the encoder. Image compression aims to reduce the file size of an image through efficient restructuring and modification of the data in an image. This, in turn, saves space as the image has been compressed in a way that makes efficient use of all the space to store data, and this results in a smaller file of the same image, which can then be transferred in less time to another device [11]. Once the file has been sent to the receiving device or needs to be accessed from storage, the compressed image is decompressed through a decoder, which decodes the encoded data and rebuilds the image. However, there is the probability that the rebuilt image might suffer from a slight data loss. Hence, the rebuilt image might not be exactly as compared to the original image. This is known as lossy compression, which happens when the rebuilt image is not the same as the original image, and lossless compression, where the rebuilt image is the same as the original image [12-17]. A flow chart of the process is shown in Figure 4.

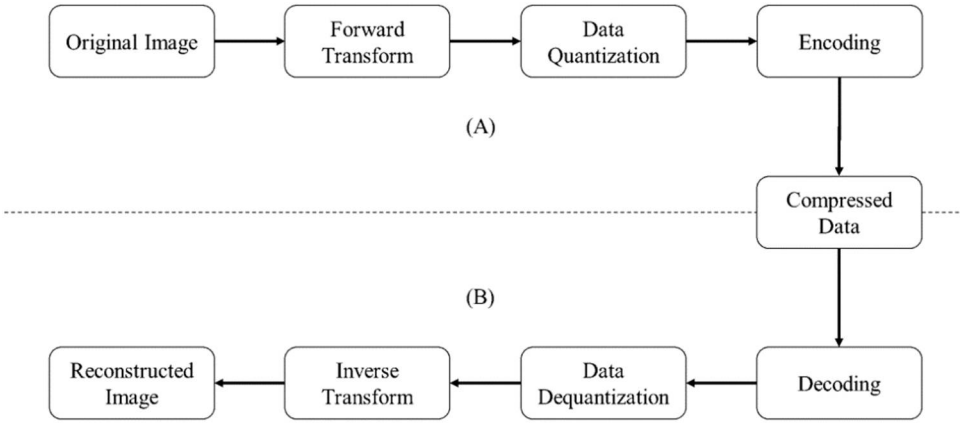

Figure 4. A general flow for (A) Image compression and (B) Image decompression systems

Near-lossless compression has come to light as the third type of compression and represents the middle ground between lossy and lossless compression. The difference between the three types of compression is in compression ratio, file size, and image quality. Lossy compression commonly produces a high compression ratio and a small file size but sacrifices image quality. On the other hand, lossless compression produces a low compression ratio and large file size, but image quality is preserved where the compressed images look exactly like the original image.

Set Partitioning in Hierarchical Trees

Set Partitioning in Hierarchical Trees (SPIHT) is a near-lossless image compression algorithm based on the Discrete Wavelet Transform (DWT) algorithm and was introduced by Amir Said and William A. Pearlman in 1996 [13, [18-20]. The SPIHT algorithm is a refined edition of the Embedded Zerotree Wavelet (EZW) algorithm. It has been widely used in regular image compression while consistently producing very good compression results compared to most other algorithms.

SPIHT compresses an image through means of recursive wavelet decomposition. At each pass, SPIHT applies a wavelet transform matrix and decomposes the data into four sub-bands, Low-Low (LL), Low-High (LH), High-Low (HL), and High-High (HH). The LH, HL, and HH sub-bands are then compared to the preset threshold level to determine whether much detail is lost in this decomposition; if it is determined that a lot of detail is lost in this decomposition pass, then the algorithm performs the next recursion pass, further refining the details until the SPIHT algorithm achieves the satisfactory threshold that only minimal detail is lost in the most recent pass.

Figure 5 depicts the process of encoding an image by applying the SPIHT algorithm. The image is first loaded into the encoder, and then the encoder reads the contents of the image. Size, resolution, bit depth, and individual pixel values are obtained.

A two-way wavelet decomposition (horizontal and vertical) is then applied to the image, and each pixel's significance is calculated. The coefficient of each pixel is then calculated to the calculated significance. From the resulting data, the coefficients are then sorted into three lists that are generated: List of Insignificant Pixels (LIP), List of Insignificant Sets (LIS), and List of Significant Pixels (LSP). The SPIHT coder then begins testing the three lists in order beginning with LIP, followed by LIS, and finally, LSP.

In the sorting pass, the coefficients in LIP are coded first. If a coefficient in the LIP becomes significant while coded, it is moved to the end of the LSP, and its signs are coded. In coding the LIS, the coefficients that become significant are partitioned into subsets, and these subsets are added to the end of the LIS, which

will also be tested and coded before the end of the current pass. Finally, each coefficient in LSP except the ones added in the last sorting pass is refined in a refinement pass. Recursion to the wavelet decomposition function is then called within each list to further refine the coefficients in each list. The process is repeated until the number of recursions achieves the allowed number of recursions N, set by the user.

The SPIHT wavelet tree of decisions is then generated by the decisions made by the coder during the parsing of the three lists. The wavelet tree can then be encoded, and as a result, the compressed data bit stream is produced. The decoding process of a SPIHT compressed data bit stream is exactly the reverse of the encoding process.

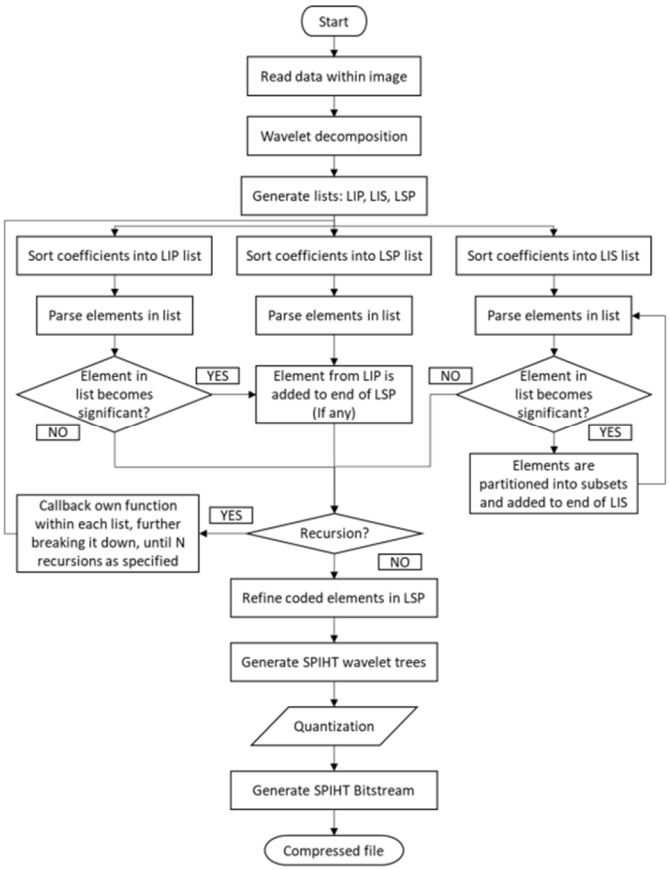

Figure 5. SPIHT encoder-decoder flow diagram

Figure 6 depicts the process of decoding an image that has been encoded using the SPIHT algorithm. First, the decoder reads the data bit stream, and the SPIHT wavelet tree is reconstructed. Then the LIP, LIS, and LSP are regenerated based on the wavelet tree. From the three lists, the coefficients of the pixels are recovered, and the wavelet decomposition is reversed to obtain the original values of the pixels. The reconstructed image can then be recovered based on the decoded info.

There can be numerous ways to evaluate a compression algorithm, whether it be through compression speed, a measure of how fast an algorithm processes an image and compresses it, through compression ratio, a measure of how much more compact the compressed image is when compared to the original file in size, through image quality, a measure of how similar is the reconstructed image when compared to the original image. These measures serve as a quantifiable measurement to evaluate the efficiency of an image compression algorithm. To measure the compression speed of an algorithm, encoding time is used, which refers to the amount of time taken, in seconds, for the encoder of a compression algorithm to encode and compress the data in the original input image into the outputted compressed data.

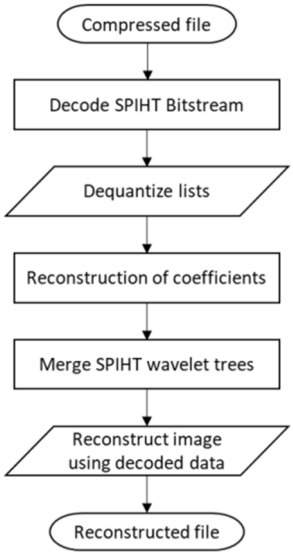

Figure 6. SPIHT encoder-decoder flow diagram

Compression Ratio (CR) refers to the ratio of bits between the original uncompressed and compressed files. It is used to measure how much space has been compressed by the algorithm in the image. For example, a CR of 4:1 signifies that the compressed image is only about 1/4th of the size of the original image. The equation to determine CR is as illustrated as follows:

$$Compression\ Ratio\ (CR) = \frac{Number\ o\ f\ Bits\ in\ Original\ Image}{Number\ o\ f\ Bits\ in\ Com\ pressed\ Image}$$

Although both are used to quantify the amount of compression that is applied to a file, CR is not to be confused with compression rate, measured in Bits Per Pixel (BPP), which represents the number of bits, on average, that is needed to represent a pixel in an image. The equation to measure BPP is as illustrated as follows:

$$Bits\ Per\ Pixel\ (BPP) = \frac{Number\ o\ f\ Bits\ in\ Image}{Number\ o\ f\ Pixel\ in\ Image}$$

There are multiple ways to measure image quality when evaluating an image compression algorithm. Peak Signal-to-Noise Ratio (PSNR) and Structural Similarity Index Measure (SSIM) are commonly used to measure image quality. PSNR is measured in decibels (dB) and represents the quality of an image relative to the size of the error, where a high PSNR value represents a low measure of error in the reconstructed image compared to the original. The equation to measure PSNR is as illustrated as follows:

$$PSNR = 10log_{10}\frac{255^2}{MSE}$$

MSE represents the Mean Squared Error, the average value of the combined square of errors, or differences in each pixel between the original and compressed image. The equation to measure MSE is as illustrated as follows:

$$MSE\ = \frac{1}{n}\sum_{i=1}^{n}\ (Y_i - Y\hat{}_i)^2$$

However, there are certain instances in which the MSE value of an image becomes inconsistent, and hence a secondary measure of image quality, SSIM, is introduced. SSIM measures image quality degradation between the original and compressed image by observing the perceivable structural differences between the two images and serves as an alternative besides PSNR for image quality measurement. The equation to measure SSIM is as illustrated as follows:

$$SSIM(x,y)\ = \frac{(2\mu x\mu y\ +\ C1)\ (2\sigma xy\ +\ C2)}{(\mu\ 2\ x\ +\ \mu\ 2\ y\ +\ C1)\ (\sigma\ 2\ x\ +\ \sigma\ 2\ y\ +\ C2)}$$

The SPIHT algorithm has been chosen for further testing and improvement from the results of the compression and parameter analysis phase, as it provides the best compression image quality with reasonable compression rates. The reconstructed image in Figure 7 shows that the reconstructed image from the SPIHT compression algorithm on the right has no distinguishable differences compared to the

original image on the left. Both color and edge details have been preserved during the SPIHT compression with no artifacts or grainy textures. This results in a reconstructed image that is not visibly different from the original image and is deemed suitable for this research. Hence, we select the SPIHT algorithm for further testing and improvement.

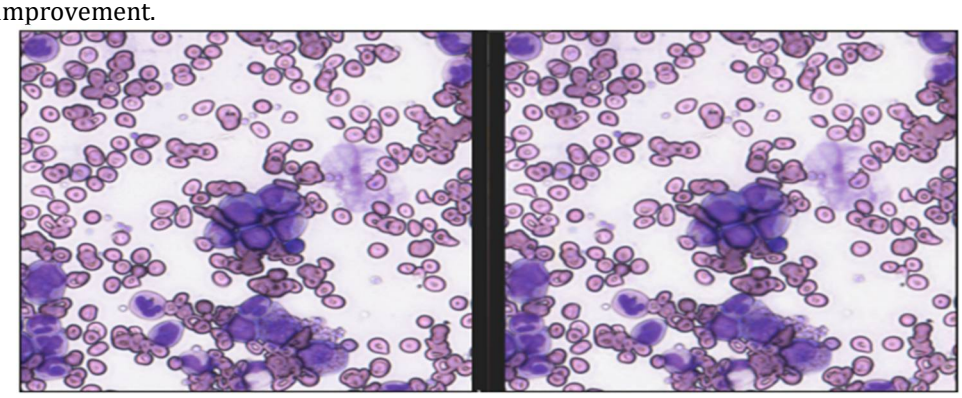

Figure 7. Original image (left) against reconstructed image through SPIHT compression (right)

SPIHT Algorithm Improvement Results

The SPIHT compression algorithm has been selected for further testing and improvement. The recursion and wavelet decomposition sections have been identified for further improvement.

Change of Wavelet in Wavelet Decomposition: A wavelet is applied by the encoder during wavelet decomposition in the SPIHT algorithm, where the applied wavelet varies from case to case and is user-defined. Common wavelet options selected for wavelet decomposition are usually from the Haar and Daubechies wavelet families, as numerous researchers have extensively used them since the early days of SPIHT, and they remain a popular option even today. In Table 1 below, a comparison between wavelets used by researchers in recent works was made by testing the algorithm on our data set.

From the results in Table 1, it can be seen that the bior4.4 wavelet variant from the Biorthogonal wavelet family produces the highest ratio of compression, with a compression ratio of 52.6860, PSNR value of 42.1882 and SSIM value of 98.0449%. In contrast, the db4 wavelet variant from the Daubechies wavelet family produces the highest quality of compression, with a compression ratio of 46.0598, PSNR value of 42.3743, and SSIM value of 98.0924%.

Table 1 Results of comparison and testing of recent works of SPIHT algorithm

Wavelet	CR	PSNR	SSIM (%)
SPIHT(bior4.4)	**52.6860**	42.1882	98.0449
SPIHT(db4)	46.0598	**42.3743**	**98.0924**
SPIHT(haar)	29.4323	41.1022	97.6950

Based on Figure 8, we can see that all three variations of the SPIHT compression algorithm produce an almost similar result in the PSNR category, with the db4 variant slightly in the lead, with a PSNR value of 42.3743 as compared to 42.1882 from the bior4.4 wavelet and 41.1022 from the Haar wavelet. Also, the bior4.4 variant produces the highest ratio of compression, at a CR value of 52.6860, whereas the haar variant produces the lowest ratio of compression, at a CR value of 29.4323.

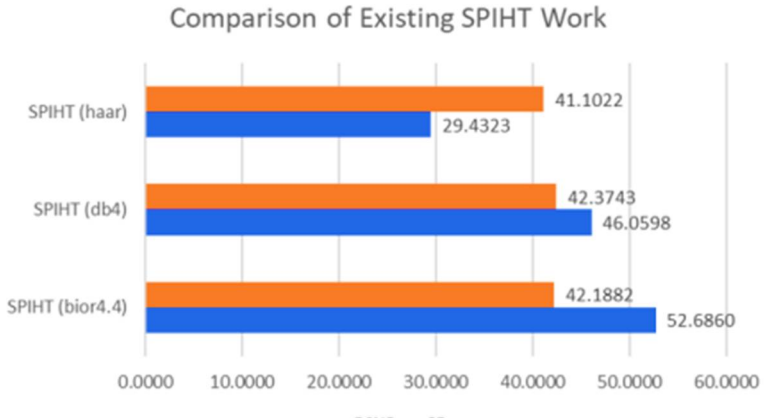

Figure 8. Results of testing of recent works of SPIHT algorithm

The wavelets are loaded into the algorithm individually, and the data set is fed through the algorithm for compression by the SPIHT algorithm with each wavelet. The data is then collected and recorded in a table. The results in Table 2 show that the SPIHT algorithm using the bior3.9 wavelet produces the best compression quality, with a PSNR value of 43.7261 dB, a higher value than that of the other wavelets. The bior3.9 wavelet also produces
a compressed image which is the most similar when compared to the original image, with an SSIM value of 98.5243% when compared to the other wavelets. This makes the bior3.9 wavelet the best-suited wavelet to be used with the SPIHT algorithm for this research, as it can produce a high-quality compressed image compared to other wavelets. Hence, we select the bior3.9 wavelet to be used as the wavelet for the proposed SPIHT algorithm.

Table 2 Results of testing different wavelets with SPIHT algorithm on high-resolution digital pathology slide scans

Wavelet	CR	PSNR	SSIM	Wavelet	CR	PSNR	SSIM
bior1.1	29.4321	41.1022	97.6950	dmey	48.8093	42.5738	98.1483
bior1.3	25.7942	41.5721	97.8183	fk14	47.7794	42.4946	98.1346
bior1.5	24.6567	41.0681	97.7154	fk18	48.2690	42.5497	98.1474
bior2.2	34.7661	42.7298	98.2409	fk22	47.8814	42.5448	98.1462
bior2.4	32.9719	43.0507	98.3232	fk4	32.7378	41.6448	97.8743
bior2.6	31.8715	43.1721	98.3545	fk6	44.2695	42.2537	98.0608
bior2.8	31.1469	43.2107	98.3625	fk8	46.4408	42.4368	98.1062
bior3.1	49.5145	40.2996	97.3876	haar	29.4323	41.1022	97.6950
bior3.3	23.3788	43.3476	98.4346	rbio1.1	29.4321	41.1022	97.6950
bior3.5	23.6553	43.6104	98.4936	rbio1.3	51.0666	41.8967	97.9456
bior3.7	23.5376	43.6207	98.5042	rbio1.5	54.8524	41.9222	97.9562
bior3.9	23.3891	**43.7261**	**98.5243**	rbio2.2	34.1890	40.0716	97.1192
bior4.4	52.6860	42.1882	98.0449	rbio2.8	57.8563	41.3367	97.7116
bior5.5	**73.7624**	41.1724	97.6855	rbio3.7	49.0508	38.9710	96.4904
bior6.8	47.3526	42.6066	98.1645	rbio3.9	52.5052	39.2638	96.6756
coif1	40.4681	42.0384	97.9884	rbio4.4	37.9748	42.4642	98.1053
coif2	46.4208	42.4226	98.1033	rbio5.5	29.0301	43.3568	98.3895
coif3	47.8477	42.4573	98.1088	rbio6.8	46.9967	42.2758	98.0634
coif4	48.2989	42.4808	98.1202	sym2	39.8918	41.9565	97.9786
coif5	48.5765	42.5224	98.1329	sym3	44.1829	42.3079	98.0662
db1	29.4324	41.1022	97.6950	sym4	45.8175	42.4016	98.0966
db10	47.7667	42.4836	98.1302	sym5	47.3930	42.4349	98.1044
db2	39.8920	41.9565	97.9786	sym6	47.3407	42.4890	98.1210
db3	44.1832	42.3079	98.0662	sym7	47.9478	42.4884	98.1224
db4	46.0598	42.3743	98.0924	sym8	47.9231	42.4951	98.1281
db5	46.7464	42.4379	98.1090				
db6	47.0461	42.4470	98.1121				
db7	47.5340	42.4781	98.1246				
db8	47.2501	42.4723	98.1250				
db9	47.5171	42.5032	98.1303				

Based on Figure 9, we can see that the bior3.9 wavelet produces the best PSNR results compared to other wavelets at a value of 43.7261 dB. Hence, we select the bior3.9 wavelet to be used as the wavelet for the proposed SPIHT algorithm.

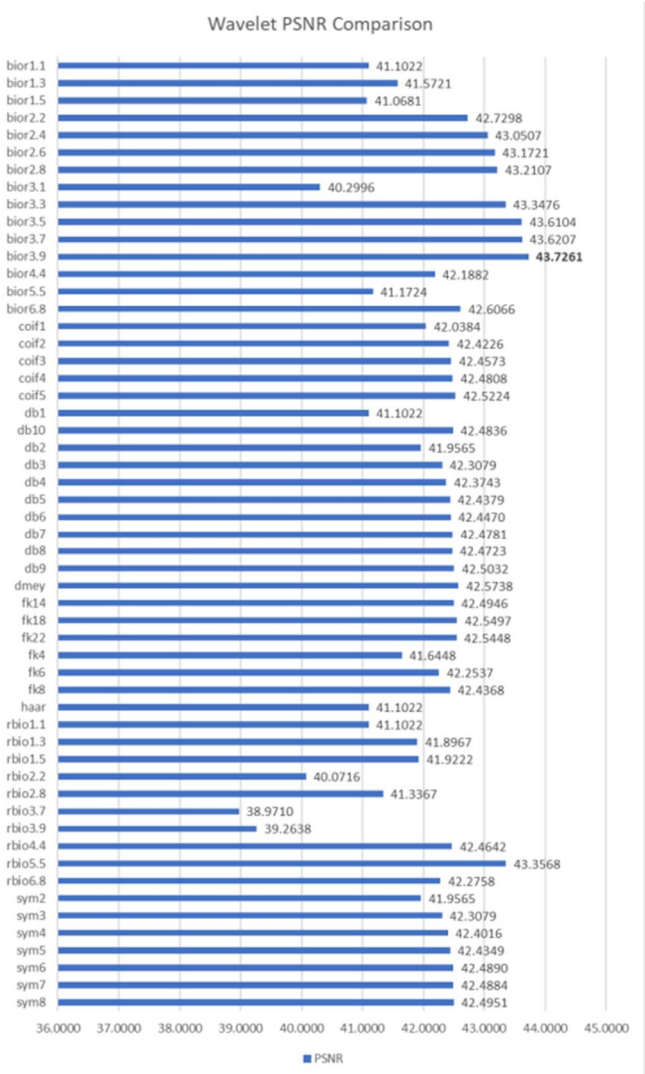

Figure 9. Results of testing proposed wavelet in SPIHT algorithm

Recursion Improvement: In the recursion function of the SPIHT compression encoder, with each recursive pass, more details are preserved, increasing the image quality. However, with each recursive pass, as more details are preserved, the compression ratio is reduced as less compression is achievable. The number of recursion passes in the algorithm is usually manually set. Still, by doing so, one does not know whether the current amount of recursion passes has reached its maximum amount of pre-servable details, nor if the current amount of recursion passes is redundant.

The results in Table 3 show a clear difference in increasing the number of recursions in the SPIHT algorithm. When the number of recursions is increased, more detail is preserved during compression, resulting in higher compression quality, but at the cost of lowered compression ratio, as more info has to be preserved in the compressed image. By applying the proposed method of automating the recursion process until the maximum recursion is achieved, we can see that both the PSNR and SSIM values have increased, with PSNR values increasing from 41.1022 to 42.1309 and SSIM values increasing from 97.6950% to 98.8446%. The increase in these values will result in a compressed image that will be an even more accurate representation of the original image.

Table 3 Results of increasing number of recursions in SPIHT algorithm

Algorithm	CR	PSNR (dB)	SSIM (%)
SPIHT	**29.4323**	41.1022	97.6950
SPIHT (Automated Recursion)	7.5301	**42.1309**	**98.8446**

Based on Figure 10, we can see that the proposed automated recursion in the SPIHT compression algorithm produces the best PSNR results compared to the other manual input recursion from previous works.

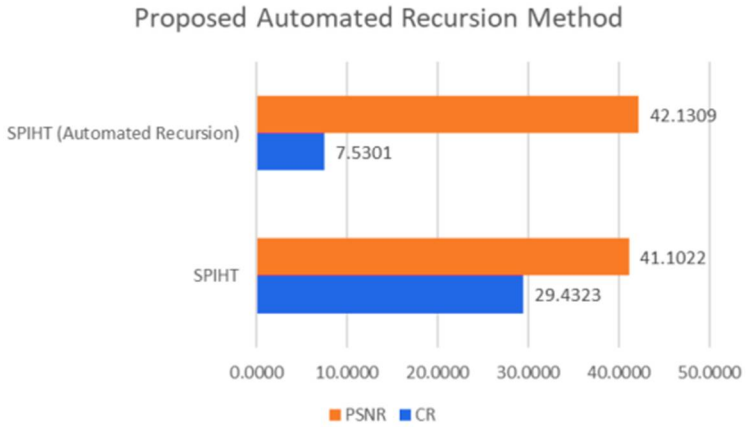

Figure 10. The results of the testing proposed an automated recursion method in the SPIHT algorithm Combination of Wavelet and Automated Recursion: By combining the proposed wavelet and the automated recursion, we expect to push the improvement in PSNR values even higher than each proposed method. We compare the proposed method against previous individual advances in SPIHT. The results of the comparison are tabulated below.

The results in Table 4 show that the proposed SPIHT algorithm has been proven to produce the best compression quality, with a PSNR value of 51.5543, a higher value than that of the other methods. It is also the most similar reconstruction to the original image, with an SSIM value of 99.8390%.

Table 4 Comparison of proposed algorithms against individual improvements

Algorithm	CR	PSNR (dB)	SSIM (%)
SPIHT	29.4323	41.1022	97.6950
SPIHT (Wavelet improvement)	23.3891	43.7261	98.5243
SPIHT (Recursion improvement)	7.5301	42.1309	98.8446
Proposed Algorithm	10.1413	**51.5543**	**99.8390**

Based on Figure 11, we can see that our proposed SPIHT compression algorithm produces the best PSNR results when compared to the individual improvements made to the SPIHT algorithm. Hence with this evaluation, we can say that the proposed improved SPIHT has proven to produce a higher quality compression when compared to its counterparts.

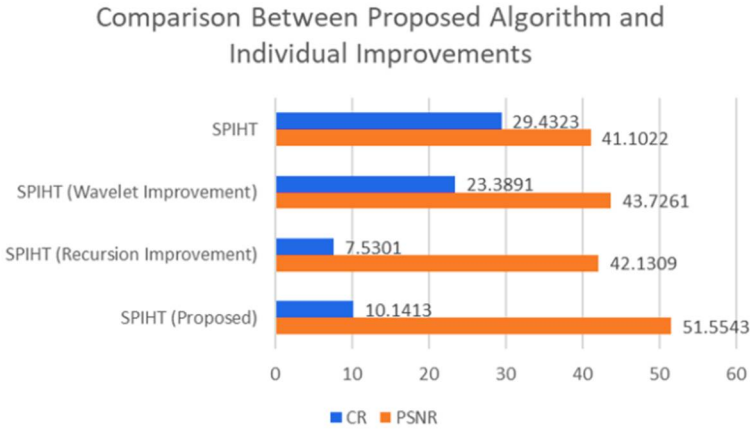

Figure 11. CR and PSNR results of testing the proposed SPIHT algorithm against individual improvements

Final Algorithm Evaluation: We compare our proposed algorithm against all other previously tested algorithms. The results in Table 5 show that the DCT algorithm produces a CR value of 57.0978, a PSNR value of 35.8207 dB, and an SSIM value of 94.4012%. The DWT algorithm produces a CR value of 320.9962, a PSNR value of 12.6927 dB, and an SSIM value of 61.5056%. The Huffman algorithm produces a CR value of 1817.7082, a PSNR value of 28.4037 dB, and an SSIM value of 85.6481%. The SPIHT algorithm uses the bior4.4 wavelet to produce a CR value of 50.2262, a PSNR value of 41.0494 dB, and an SSIM value of

98.3836%. The SPIHT algorithm that uses the db4 wavelet produces a CR value of 45.9440, a PSNR value of 41.1340 dB, and an SSIM value of 98.4145%. The SPIHT algorithm that uses the haar wavelet produces a CR value of 30.9884, a PSNR value of 40.3577 dB, and an SSIM value of 98.2298%. Lastly, we can see that the proposed SPIHT algorithm has been proven to produce the best compression quality, with a PSNR value of 51.5543 dB, a higher value than that of the other methods. It is also the most similar reconstruction to the original image, with an SSIM value of 99.8390%, albeit with a lower CR value of 10.1413.

Table 5 Comparison of algorithms tested against the proposed SPIHT algorithm

Algorithm	CR	PSNR (dB)	SSIM (%)
DCT	57.0978	35.8207	94.4012
DWT	320.9962	12.6927	61.5056
Huffman	**1817.7082**	28.4037	85.6481
SPIHT(bior4.4 Miya)	52.6860	42.1882	98.0449
SPIHT(db4 Sran)	46.0598	42.3743	98.0924
SPIHT(haar Miya)	29.4323	41.1022	97.6950
Proposed Algorithm	10.1413	**51.5543**	**99.8390**

Based on Figure 12, we can see that our proposed improvements for the SPIHT compression algorithm produce a high PSNR result compared to other image compression algorithms, at a value of 51.5543 dB. The proposed algorithm produced better PSNR results when compared to different algorithms, with DCT at 35.8207 dB, DwT at 12.6927 dB, and Huffman at 28.4037 dB. Hence with this evaluation, we can say that the proposed improved SPIHT has produced a higher quality compression compared to other image compression algorithms to compress high-resolution digital pathology slide scans. The proposed algorithm also achieved higher PSNR values than previous works in SPIHT, with the proposed method achieving PSNR values of 42.1882 dB and 41.1022 dB, respectively. In comparison, the proposed method achieved a PSNR value of 42.3743 dB, while the proposed algorithm achieved a PSNR value of 51.5543 dB.

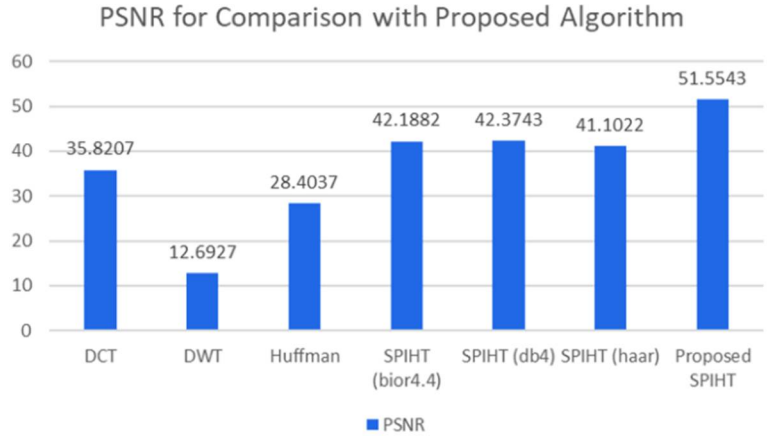

Figure 12. PSNR results of testing the proposed SPIHT algorithm against other algorithms

CONCLUSION

In conclusion, the results from this research support the idea that the proposed near lossless auto recursive SPIHT-based image compression algorithm for high-resolution digital pathology images can produce a compressed image of a higher quality than that of the SPIHT algorithm and also does not suffer from any significant visually discernible detail loss when compared to the original image, from a pathologist's point of view. Further research can be done to increase the compression capabilities to improve the algorithm's compression ratio while maintaining the current image quality.

REFERENCES

1. M. Ferroukhi, A. Ouahabi, M. Attari, Y. Habchi, and A. Taleb-Ahmed, (2019). "Medical video coding based on 2nd-generation wavelets: Performance evaluation," *Electronics,* vol. 8, no. 1, p. 88.
2. H. Vohra *et al.*, (2022). "A Low Overhead and Scalable Authentication and Encryption Scheme for Medical Wireless Sensor Networks."pp98.
3. Y. Liu, X. Zhou, and W. Zhong, (2023). "Multi-Modality Image Fusion and Object Detection Based on Semantic Information," *Entropy,* vol. 25, no. 5, p. 718,

4. S. Boopathiraja, V. Punitha, P. Kalavathi, and V. S. Prasath, (2022). "Computational 2D and 3D medical image data compression models," *Archives of Computational Methods in Engineering,* vol. 29, no. 2, pp. 975-1007.
5. L. J. Ahmed, B. A. Fathima, M. Mahaboob, and B. Gokulavasan, (2021). "Biomedical Image Processing with Improved SPIHT Algorithm and optimized Curvelet Transform Technique," in *2021 7th International Conference on Advanced Computing and Communication Systems (ICACCS)*, vol. 1: IEEE, pp. 1596-1602.
6. D. S. Laiphrakpam, L. S. Waikhom, D. Brahma, P. Baruah, and S. Biswas, (2021). "Image compression–encryption scheme using SPIHT and chaotic systems," *Journal of Information Security and Applications,* vol. 63, p. 103010.
7. S. Boopathiraja, P. Kalavathi, S. Deoghare, and V. S. Prasath, (2023). "Near Lossless Compression for 3D Radiological Images Using Optimal Multilinear Singular Value Decomposition (3D-VOI-OMLSVD)," *Journal of Digital Imaging,* vol. 36, no. 1, pp. 259-275.
8. M. A. Elaveini and T. Deepa, (2023). "Hybrid Transform Based Compressive Sensing of Image with Better Quality Using Denoising Convolution Neural Network," *Wireless Personal Communications,* vol. 128, no. 1, pp. 645-663.
9. T. M. Godinho, R. Lebre, L. B. Silva, and C. Costa, (2017). "An efficient architecture to support digital pathology in standard medical imaging repositories," *Journal of biomedical informatics,* vol. 71, pp. 190-197.
10. M. D. Zarella *et al.*, (2019). "A practical guide to whole slide imaging: a white paper from the digital pathology association," *Archives of pathology & laboratory medicine,* vol. 143, no. 2, pp. 222-234.
11. N. Azman, S. Ali, R. A. Rashid, F. A. Saparudin, and M. A. Sarijari, (2019). "A hybrid predictive technique for lossless image compression," *Bulletin of electrical engineering and informatics,* vol. 8, no. 4, pp. 1289-1296.
12. M. A. Rahman and M. Hamada, (2019). "Lossless image compression techniques: A state-of-the-art survey," *Symmetry,* vol. 11, no. 10, p. 1274.
13. A. Said and W. A. Pearlman, (1996). "A new, fast, and efficient image codec based on set partitioning in hierarchical trees," *IEEE Transactions on circuits and systems for video technology,* vol. 6, no. 3, pp. 243-250.
14. Varish N, Hasan MK, Khan A, Zamani AT, Ayyasamy V, Islam S, Alam R. (2023). Content-Based remote sensing image retrieval method using adaptive tetrolet transform based GLCM features. Journal of Intelligent & Fuzzy Systems. 1-24.
15. Albadr MA, Ayob M, Tiun S, Al-Dhief FT, Hasan MK. (2022). Gray wolf optimization-extreme learning machine approach for diabetic retinopathy detection. Frontiers in Public Health.1;10:925901.
16. Varish N, Pal AK, Hassan R, Hasan MK, Khan A, Parveen N, Banerjee D, Pellakuri V, Haqis AU, Memon I. (2020). Image retrieval scheme using quantized bins of color image components and adaptive tetrolet transform. IEEE Access.;8:117639-65.
17. Junchai G, Keding Y, Bing H, Hashim W, Ahmad AH, Ismail AF, Yau KL, Hasan MK, Yahya NA, Hong Z, Xianzhou F. (2017). Imaging Monocular Vision Localization and Application in Smart Home. International Journal of Smart Home. 11(2):1-6.
18. Ghazal, Taher M., et al. (2023). "An integrated cloud and blockchain enabled platforms for biomedical research." The Effect of Information Technology on Business and Marketing Intelligence Systems. Cham: Springer International Publishing, 2037-2053.
19. Dhasarathan C, Hasan MK, Islam S, Abdullah S, Mokhtar UA, Javed AR, Goundar S. (2023). COVID-19 health data analysis and personal data preserving: A homomorphic privacy enforcement approach. Computer communications. 1;199:87-97.
20. Siddiqui SY, Haider A, Ghazal TM, Khan MA, Naseer I, Abbas S, Rahman M, Khan JA, Ahmad M, Hasan MK, Ateeq K. (2021). IoMT cloud-based intelligent prediction of breast cancer stages empowered with deep learning. IEEE Access. ;9:146478-91.

CITATION OF THIS ARTICLE

Goh J Y, Afzan A, Mohammad K H, AKM Ahasan H, Zaid Abdi A A, Mohammad F A F, Elaine W L C. SPIHT Image Compression Algorithm for High-Precision Digital Images. Bull. Env. Pharmacol. Life Sci., Vol 12[10] September 2023: 128-139.